

## Studies of Small Molecule Dyes that Interact with Pyrene-labeled Amyloid Fragments

Hyemin Lee, Hwiin Lee, and Minyung Lee\*

Department of Chemistry and Nanoscience Global Top 5 Research Program, Ewha Womans University, Seoul 120-750, Korea

\*E-mail: mylee@ewha.ac.kr

Received April 29, 2014, Accepted July 26, 2014

**Key Words** : Pyrene fluorescence, Excimer, Dye screening, Amyloid dimer

Certain dyes and pigments are promising candidates for disease therapeutics. Specifically, many of these dyes (or pigments) have shown inhibitory effects on amyloid- $\beta$  ( $A\beta$ ) aggregation, which appears to be a primary cause of Alzheimer's disease. Such examples include polyphenols, curcumin, benzothiazoles, porphyrins, and coumarin derivatives.<sup>1</sup> These small molecules are highly efficient for blocking the formation of  $A\beta$  oligomers or fibrils. Full length  $A\beta$ , consisting of 39-43 amino acid sequences, contains an aggregation motif called the central hydrophobic core (CHC).<sup>2</sup>  $A\beta$  fragments, rather than full length  $A\beta$ , have often been used in order to focus more sharply on the aggregation motif. Some examples include  $A\beta_{16-22}$ ,  $A\beta_{1-28}$ ,  $A\beta_{11-25}$ ,  $A\beta_{21-30}$ , and  $A\beta_{10-35}$ .<sup>3</sup>

Among the  $A\beta$  fragments, the physical properties of  $A\beta_{11-25}$  have been well characterized. The fibril structure of  $A\beta_{11-25}$  was first determined by X-ray crystallography<sup>4</sup> and solid-state NMR.<sup>5</sup> On the basis of its structural information,  $A\beta_{11-25}$  was subjected to fluorescence resonance energy transfer (FRET) and conformational switching of the FRET peptide was observed in the course of oligomerization.<sup>6</sup> The stability and microscopic structures of the fragment were further investigated by employing molecular dynamics simulations.<sup>7,8</sup> The researchers showed that the CHC aggregation motif that amounts to the amino acid sequence of LVFFA plays a key role in the  $A\beta_{11-25}$  aggregation process. The main objective of this work was to identify dyes that interfere with the CHC and thus inhibit aggregation. Dye-amyloid interactions were monitored by employing excimer (excited dimer) fluorescence. We attached pyrene to the N-terminus of  $A\beta_{11-25}$  and observed its monomer and excimer fluorescence.

$A\beta$  dimers are a more desirable target than oligomers because dimer formation represents the first step of  $A\beta$  assembly into toxic oligomers. The excimer fluorescence of Py- $A\beta_{11-25}$  provides detailed information on the dimer formation process that facilitates studies of the early-stage aggregation of the fragment. We measured the excimer/monomer fluorescence ratios using this platform for six dyes by examining pyrene excimer fluorescence as a function of the dye concentration. We attempted to delineate the dye-amyloid interactions in terms of the inhibition efficiency and showed that the pyrene-labeled amyloid probe can be used as a simple model system to study interactions between dyes and peptides.

Upon UV excitation, the emission spectrum of the pyrene monomer exhibited several sharp peaks (370 to 430 nm). In contrast, the pyrene excimer fluorescence appeared as a broad,

unstructured band at longer wavelengths (ranging from 425 to 550 nm, centered at approximately 460 nm) than those of the monomer. The maxima of the two entities were well separated, allowing both fluorescence peaks to be easily discerned.<sup>9,10</sup> On the basis of *in cerebro* screening, we subjectively selected organic dyes that exhibit virtually no fluorescence with the UV excitation wavelength but interact with the  $A\beta_{11-25}$  dimer. Figure 1 shows the molecular structures of the six candidates that were hypothesized to satisfy such criteria. These molecules exhibit very low fluorescence quantum yields due to ultrafast nonradiative relaxation in the excited state.<sup>11</sup>

Curcumin (compound **1**) is a naturally occurring yellow-orange pigment found in the rhizomes of the herb *Curcuma longa*. Curcumin is responsible for the bright yellow color of turmeric and has been extensively used as a spice, with potential applications as an antioxidant and anticancer agent.<sup>12-14</sup> Hemin (compound **2**) is an important physiological mediator of ion channel stimulation and intracellular communication.<sup>15-17</sup> Azobenzene derivatives (compounds **3-6**) belong to push-pull type molecules where the amino group acts as an electron donor and the nitro group acts as an electron acceptor.<sup>15</sup> Disperse orange 3 (DO3) has been known to exhibit high nonlinear optical properties. Disperse red 1 (DR1) is a modified form of DO3 functionalized with amino group for labeling purposes.<sup>18</sup> Methyl red (MR) is frequently used as a pH indicator, and Basic blue 41 (BB41) is a well-known coloring agent.

Pyrene has a high molar extinction coefficient ( $\epsilon_{\max} \approx 5 \times 10^4 \text{ M}^{-1}\text{cm}^{-1}$ ) in the near UV region and a moderately high fluorescence quantum yield. The monomer fluorescence is highly structured with several vibronic bands. Unlike many other dyes, the absorption and emission spectra of pyrene do not overlap because the  $S_1 \leftarrow S_0$  transition is symmetry-forbidden.<sup>19</sup> When an excited pyrene encounters a ground-state pyrene, the excitation energy is delocalized through the  $\pi$ -stacking of the dimer, resulting in excimer fluorescence.<sup>20</sup> The excimer features a broad, structureless emission band that occurs at longer wavelengths than that of the monomer. The dimerization of Py- $A\beta_{11-25}$  is not only controlled by solution diffusion but also by peptide association. The excimer of Py- $A\beta_{11-25}$  is formed when two pyrenes are in spatial proximity and two peptides are in optimal geometry under conformationally favorable conditions.

Our experiments were performed in an acidic buffer (pH

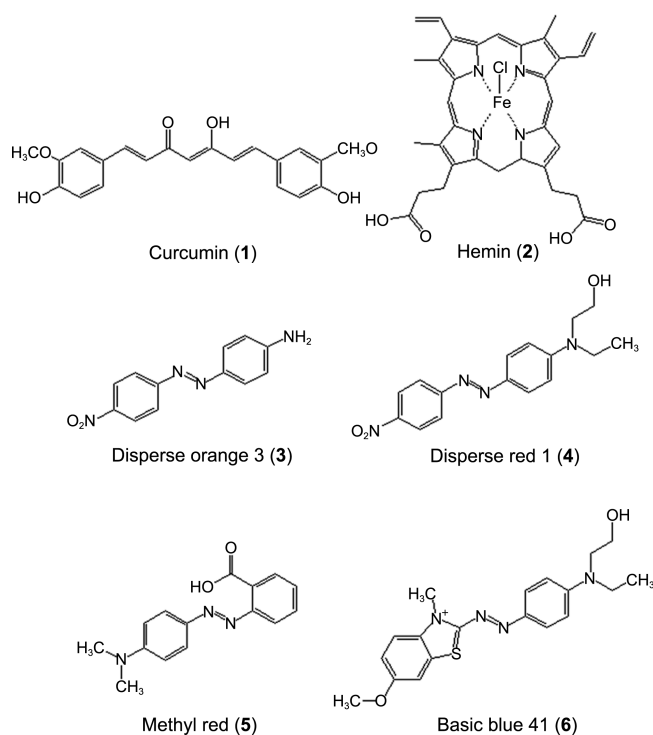


**Figure 1.** The molecular structures of potential inhibitors.

5.2, sodium acetate buffer), where the aggregation process of A $\beta$ <sub>11-25</sub> is faster than that under other pH conditions. Figure 2 shows the fluorescence spectra of Py-A $\beta$ <sub>11-25</sub> at pH 5.2 in the absence and in the presence of small molecules (Thioflavin T (ThT) and hemin).

The concentrations of both compounds were 800 nM, four times higher than that of Py-A $\beta$ <sub>11-25</sub>. The control shows the characteristic excimer band; the well-known ThT does not exhibit any inhibitory effect, indicating that ThT does not interact with the Py-A $\beta$ <sub>11-25</sub> dimer. Electronically excited ThT in liquid instantly undergoes an internal twisting that acts as an ultrafast nonradiative decay channel.<sup>21-23</sup> When bound to amyloid fibrils, the fluorescence intensity of ThT markedly increases due to the retardation of the excited

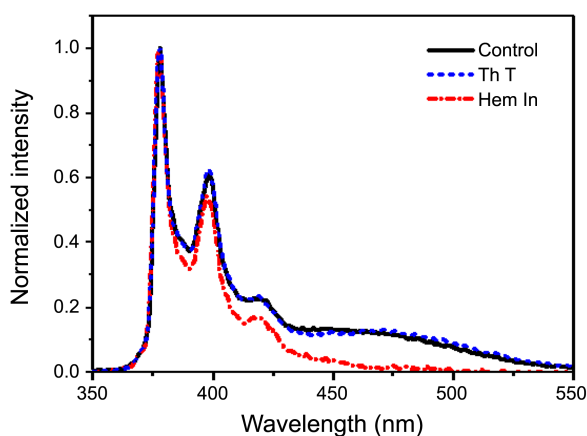


**Figure 2.** A fluorescence Py-A $\beta$  in the presence of ThT and hemin.

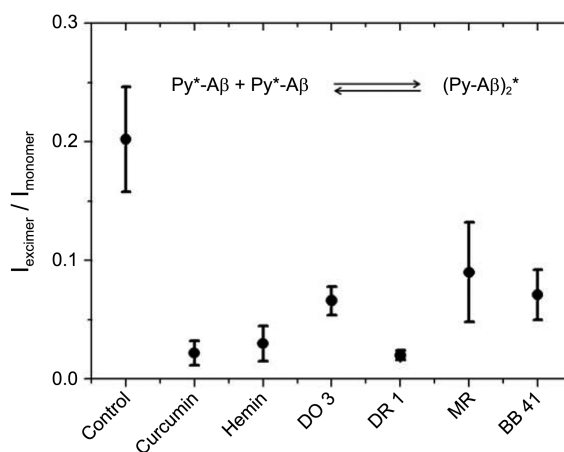


**Figure 3.** The excimer-to-monomer ratio (IE/IM) of Py-A $\beta$ <sub>11-25</sub> fluorescence at the fixed concentration (800 nM) of the dyes.

motion.<sup>23</sup> Recently, the fluorescence of ThT has been shown to be sensitive to large oligomers.<sup>24</sup> Such a rigidity-sensitive dye cannot be used to detect dimers because dimers cannot provide sufficient rigidity for a fluorescence increase. In comparison with ThT, hemin almost completely abolished the excimer fluorescence under this concentration, indicating that hemin interacts strongly with the amyloid dimer. The data prove that the excimer of Py-A $\beta$  can be effectively used to search for dyes that interfere with amyloid dimerization.

Figure 3 shows the excimer-to-monomer ratio (IE/IM) of Py-A $\beta$ <sub>11-25</sub> fluorescence at a fixed concentration (800 nM) of the dyes. The lower value of IE/IM indicates a higher inhibition efficiency. The data showed that the six dyes are all aggregation inhibitors, not promoters. Curcumin was also thoroughly investigated *in vitro* and *in vivo* for its inhibitory effect on amyloid aggregation. However, its usage for amyloidosis is limited due to its poor aqueous solubility and low pH stability. Hemin has been known to block the formation of A $\beta$  aggregates. Howlett *et al.* investigated the inhibitory effect of hemin and related porphyrins on amyloid

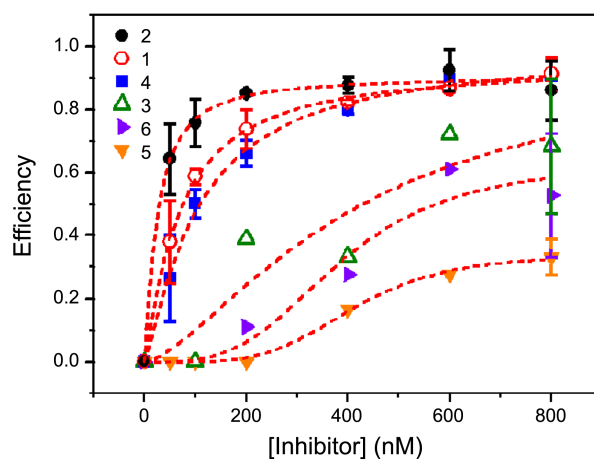


**Figure 4.** The inhibition efficiency as function of the inhibitor concentration.

aggregation using an oligomer-targeted immunoassay.<sup>15</sup> They observed that iron porphyrins, hemin, and hematin are powerful inhibitors of A $\beta$  aggregation. Our data clearly show that hemin participates in aggregation inhibition at the dimer stage. Binding studies were also performed for four azobenzene derivatives (DO3, DR1, MR, and BB41); these derivatives were of interest because Congo red,<sup>25-26</sup> a well-known azobenzene derivative, has long been used as an amyloid aggregate probe. Our data show that the azobenzene derivatives exhibit relatively high binding abilities to the dimers with some degree of variance.

Further experiments were performed with the six dyes at various concentrations in the range of 0 to 800 nM. Figure 4 shows the inhibition efficiency as a function of the inhibitor concentration. The sigmoidal curves were fitted to the following equation to calculate the IC<sub>50</sub>.

$$y = \frac{A - D}{1 + \left(\frac{x}{C}\right)^B} + D \quad (1)$$

where  $D$  is the efficiency corresponding to the flat part of the curve at high concentrations, and  $A$  is the efficiency corresponding to the asymptote at low concentrations. The coefficient  $C$  is the concentration at the mid-point between  $A$  and  $D$ , commonly called the IC<sub>50</sub>. The calculated values of IC<sub>50</sub> using Eq. (1) are given in Table 1, where a lower value indicates higher binding affinity. Among the six dyes, hemin showed the highest binding affinity, with an IC<sub>50</sub> value of 24.6 nM. Curcumin and DR1 also showed marginally good binding affinities with the value IC<sub>50</sub> of 68.2 nM and 105.8 nM, respectively. The remaining three azobenzene derivatives exhibited relatively low binding affinities. In general, amyloid oligomerization is a multi-step process and dimer formation (excimer) amounts to the earliest stage. Our results show that our assay system based on pyrene excimer fluorescence provides a viable method of exploring small molecule dyes that efficiently block early stage amyloid aggregation. However, we cannot rule out the possibility that excimer fluorescence can be quenched by small molecule dyes through fluorescence resonance energy transfer. In addition, the reason why hemin shows the highest binding efficiency is unknown. It may require further detailed work, based on intermolecular interactions between amyloid and hemin.

In conclusion, we employed an assay system using pyrene

fluorescence to study the early stage aggregation of A $\beta$ <sub>11-25</sub>. The excimer formation of A $\beta$ <sub>11-25</sub> makes it possible to perform a dimer-based assay for the amyloid aggregation process. ThT did not significantly affect excimer fluorescence, confirming that ThT participates in the late stage aggregation. Curcumin showed an efficient anti-aggregation effect on early-stage A $\beta$  aggregates. The inhibitory efficiencies of the azobenzene derivatives depended on their molecular structures. Among these, hemin exhibited the highest binding affinity to dimeric A $\beta$ . This work shows that dye screening using pyrene excimer fluorescence is an efficient way to search for dyes that block amyloid aggregation at the early stage.

## Experimental

Curcumin was obtained from Enzo Life Science (purity > 98.5%). Thioflavin T (ThT), hemin, disperse orange 3 (DO 3), disperse red 1 (DR 1), methyl red (MR), and basic blue 41 (BB 41) were supplied from Sigma-Aldrich. Amine reactive pyrene (1-pyrenebutyric acid *N*-hydroxysuccinimide ester) was covalently labeled to the *N*-terminus of A $\beta$ <sub>11-25</sub> (Py-A $\beta$ , purity > 95% HPLC) at Pepton, Inc. A 1 mM stock solution of Py-A $\beta$ <sub>11-25</sub> was prepared in DMSO and then diluted in 10 mM sodium acetate buffer at a concentration of 200 nM. The final concentrations of the inhibitory candidates were in the range of 0 to 800 nM in a total volume of 2 mL.

The fluorescence spectra were obtained using a spectrofluorometer (F-7000, Hitachi). The samples were excited at 335 nm and the emission spectra were collected in the range of 350–550 nm. A two-channel fluorescence detection system was built to monitor the intensities of the monomer and excimer fluorescence simultaneously. A UV lamp (Ocean optics) was used as the light source, centered at a wavelength of 335 nm, and delivered through an optical fiber to a 1 cm quartz sample cuvette. Emitted photons were detected at the two right angles. Each arm contains 386 nm and 500 nm band pass filters (FWHM 30 nm, Semrock) for monomer and excimer fluorescence detection, respectively. The fluorescence photons detected by two PMTs (TBX-04, HORIBA) were recorded by a two channel photon counter, where Channel 1 and Channel 2 were set for the monomer and excimer, respectively.

The blank-subtracted photons from each channel were counted and the inhibition efficiency was calculated from the ratio of  $I_{\text{excimer}}/I_{\text{monomer}}$ . The inhibition efficiency was defined as  $(I_0 - I)/I_0$ , where  $I_0$  and  $I$  correspond to the ratio of  $I_{\text{excimer}}/I_{\text{monomer}}$  of the control and the candidate, respectively. Then, the half-maximal inhibitory concentration (IC<sub>50</sub>) was calculated for each candidate as a measure of the inhibition efficiency.

**Acknowledgments.** This research was supported by the Basic Science Research Program through the National Research Foundation of Korea funded by the Ministry of Education (NRF-2013R1A1A2A10004510).

**Table 1.** The inhibitory constant (IC<sub>50</sub>) obtained by fitting the sigmoidal curves (efficiency vs. concentration of candidates). The correlation coefficients (R<sup>2</sup>) are also shown

No	Candidates	IC <sub>50</sub> (nM)	R <sup>2</sup>
1	Curcumin	68.2	0.998
2	Hemin	24.6	0.994
3	DO3	416.2	0.790
4	DR1	105.8	0.996
5	MR	413.1	0.995
6	BB41	385.7	0.871

## References

1. Sigurdsoon, E. M.; Calero, M.; Gasset, M. *Amyloid Proteins: Methods and Protocols*, 2nd ed.; Springer: 2012.
  2. Hamley, I. W. *Chem. Rev.* **2012**, *112*, 5147.
  3. Otzen, D. E. *Amyloid Fibrils and Perifibrillar Aggregates: Molecular and Biological Properties*; Wiley-VCH: Germany, 2013; p 102.
  4. Sikorski, P.; Atkins, E. D.; Serpell, L. C. *Structure* **2003**, *11*, 915.
  5. Petkova, A. T.; Buntkowsky, G.; Dyda, F.; Leapman, R. D.; Yau, W. M.; Tycko, R. *J. Mol. Biol.* **2004**, *335*, 247.
  6. Kim, J.; Lee, M. *Biochem. Biophys. Res. Commun.* **2004**, *316*, 393.
  7. Boucher, G.; Mousseau, N.; Derreumaux, P. *Proteins* **2006**, *65*, 877.
  8. Negureanu, L.; Baumketner, A. *J. Mol. Biol.* **2009**, *389*, 921.
  9. Lehrer, S. S. *Biochem.* **1995**, *24*, 115.
  10. Bains, G.; Patel, A. B.; Narayanawami, V. *Molecules* **2011**, *16*, 7909.
  11. Lakowicz, J. R. *Principles of Fluorescence Spectroscopy*, 3rd ed.; Springer: 2006.
  12. Yang, F.; Lim, G. P.; Begum, A. N.; Ubeda, O. J.; Simmons, M. R.; Ambegaokar, S. S.; Chen, P. P.; Kaye, R.; Glabe, C. G.; Frautsch, S. A.; Cole, G. M. *J. Biol. Chem.* **2005**, *280*, 5892.
  13. Anand, P.; Kunnumakkara, A. B.; Newman, R. A.; Aggarwal, B. B. *Mol. Pharmaceutics* **2007**, *4*, 807.
  14. Priyadarsini, K. I. *J. Photochem. Photobiol. C* **2009**, *10*, 81.
  15. Howlett, D.; Cutler, P.; Heales, S.; Camilleri, P. *FEBS Lett.* **1997**, *417*, 249.
  16. Li, B.; Qin, C.; Wang, L.; Dong, S. *Anal. Chem.* **2009**, *81*, 3544.
  17. Chuang, J. Y.; Lee, C. W.; Shih, Y. H.; Yang, T.; Yu, L.; Kuo, Y. M. *PLoS One* **2012**, *7*, e33120.
  18. Bandara, H. M.; Burdette, S. C. *Chem. Soc. Rev.* **2012**, *41*, 1809.
  19. Matveeva, E. G.; Rudolph, A.; Moll, J. R.; Thompson, R. B. *ACS Chem. Neurosci.* **2012**, *3*, 982.
  20. Duhamel, J. *Langmuir* **2012**, *28*, 6527.
  21. Khurana, R.; Coleman, C.; Ionescu-Zanetti, C.; Carter, S. A.; Krishna, V.; Grover, R. K.; Roy, R.; Singh, S. *J. Struct. Biol.* **2005**, *151*, 229.
  22. Krebs, M. R. H. *J. Struct. Biol.* **2005**, *149*, 30.
  23. Levine, H. *Amyloid* **2007**, *14*, 185.
  24. Maezawa, I.; Hong, H.; Liu, R.; Chun, W.; Cheng, R. H.; Kung, M.; Kung, H.; Lam, K.; Oddo, S.; La, F. M.; Lee, J. *J. Neurochem.* **2008**, *104*, 458.
  25. Hamaguchi, T.; Ono, K.; Yamada, M. *Cell Mol. Life Sci.* **2006**, *63*, 1538.
  26. Necula, M.; Kaye, R.; Milton, S.; Glabe, C. G. *J. Biol. Chem.* **2007**, *282*, 10311.
-